

## A NUMERICAL SOLUTION FOR FLUID FLOW IN UNSATURATED POROUS MEDIUM (SOIL)

RAMESH CHANDRA TIMSINA<sup>1</sup>

<sup>1</sup> *Department of Mathematics, Patan Multiple Campus, Tribhuvan University,*

*Kathmandu, Nepal*

*email : timsinaramesh72@yahoo.com*

**Abstract:** We solve the two - dimensional mixed form Kirchhoff transformed Richards equation numerically using Crank - Nicolson scheme. This procedure has been integrated using cylindrical coordinates in an axially symmetric diffusion of flow in a homogeneous, isotropic porous medium. The soil has uniform hydraulic conductivity and no source or sink. The framework is cylindrical with a finite difference structured mesh. This procedure is particularly targeted at infiltration into dry soil, drainage, perched water table and flow through homogeneous materials. However, it is also applicable to any process involving flow through porous medium. The scheme we used is more accurate, comprehensive and is computationally efficient. It may provide a suitable basis for the implementation in large scale.

**Keywords:** Porous medium, Finite difference method, Richards Equation, Kirchhoff Transformation, Infiltration.

### 1. INTRODUCTION

The unsaturated zone is the region between the soil surface and the groundwater table where many physical phenomena, such as infiltration, evaporation, groundwater recharge, soil moisture storage, and others, take place. In recent years, predicting fluid movement in this zone has become an emerging problem in soil mechanics (rainfall-induced landslides, floods, etc.), fluid mechanics, agricultural engineering, environmental engineering, and other fields. The flow in the unsaturated zone involves a two-phase flow of air and water. Since the air phase is continuous and at atmospheric pressure, we consider only the flow of water. For transient two-dimensional flow in an isotropic and homogeneous medium, the governing equations are Darcy's law and the mass conservation law. Darcy's law relates the flow velocity of water to the gradient of hydraulic potential, and the mass conservation law ensures that the total mass of water in the system remains constant. Additionally, we neglect osmotic and thermo-osmotic effects and assume that water density varies only with capillary pressure. Under these assumptions, the fluid motion obeyed the classical Richards equation.

Different forms of Richards equation can be written with  $\psi$  (the pressure head), or  $\theta$  (the volumetric moisture content) as the dependent variable. We consider the Richards equation in the following (mixed) form with no source as [1].

$$(1.1) \quad \frac{\partial \theta}{\partial t} - \nabla \cdot (K(\psi) \nabla \psi) + \frac{\partial K}{\partial z} = 0,$$

where  $\theta$  (the volumetric moisture content),  $\psi$  (the pressure head),  $K(\psi)$  is the unsaturated hydraulic conductivity

We prefer the constitutive relationship between  $\theta = \theta(x, y, z, t)$  and  $\psi = \psi(x, y, z, t)$  due to by Haverkamp et al. [2] allows to express the Richards equation (1.1) with a single dependent variable  $\psi$  or  $\theta$ .

The hydraulic conductivity  $K(\psi)$  describes the ease with which water can move through pore space, and depends on the intrinsic permeability of the material and the properties of fluid such as degree of saturation, density and the viscosity [3]. There are many empirical formulations for the hydraulic conductivity  $K(\psi)$  and the moisture content  $\theta(\psi)$  functions. We use the following popular model from groundwater hydrology due to Haverkamp et al. [2] and express these constitutive relations as the continuous functions of  $\psi$ .

$$(1.2) \quad K(\psi) = K_s \frac{A}{\alpha + |\psi|^\gamma}, \quad \theta(\psi) = \theta_r + \frac{\alpha(\theta_s - \theta_r)}{\alpha + |\psi|^\beta},$$

where  $\theta_s = 0.287$  and  $\theta_r = 0.075$  represent the saturated and residual moisture content respectively,  $K_s = 34$  corresponds to the saturated hydraulic conductivity, and  $A = 1.175 \times 10^6$ ,  $\alpha = 1.611 \times 10^6$ ,  $\beta = 3.96$ ,  $\gamma = 4.74$  are dimensionless soil parameters. These data are used to describe the infiltration process in soil.

Richards equation is highly nonlinear partial differential equation. Because of its nonlinear behavior, analytic solutions are limited to some simplified cases with no practical importance. Hence numerical approximations are used to solve the unsaturated flow equation. Approximated solutions are computed using discretization methods that depends on approximation techniques for space and time derivatives, and the solution method for the nonlinear system of discretization equations. The standard approximations that are applied to the spatial domain are finite difference, finite element and finite volume methods. They are usually applied on a fixed spatial grid and also in an adaptive approach. The standard temporal derivative approximation method is the Euler method. Picard, modified Picard, and Newton methods are the most frequently used methods to deal with the nonlinearity of the Richards equation [4]. The linearization of Richards equation yields to a system of linear algebraic equations which is typically solved by using direct method for one dimensional problem and iterative approach for large linear systems arising from higher dimension problems.

The numerical solution of Richards equation is still a subject of great interest, mainly, on focusing to the reduction of computational cost to achieve the robust and more accurate solution. In addition, real world application requires the combine analysis with soil moisture dynamics with contamination transport, growth and decay of microorganisms in transport phenomenon, energy balance and rain runoff which make the computational problem of

solving the Richards equation more complex. To avoid such type of stumbling block the solution techniques of Richards equation have to be extended, to much large computational domains and implementing to high performance computing code.

## 2. BACKGROUND

Numerical solutions of Richards equation has a significant history in the fields of soil science and ground water hydrology. General overviews and thorough reviews of the literature may be found in the works of Nielsen et al. and Milly [5, 6]. Generally, numerical solutions are either the  $h$ -based or  $\theta$ -based form of Richards equation. A number of finite difference, finite element and finite volume solution schemes [2][7, 8, 9, 10, 11, 12] have been used for the simulation of these form of the equation. To drive the numerical simulation in mixed form of Richards equation [4, 13] play an important role in the history of soil science. They used collation approximation in space and an alternating-direction version namely a "quasi-Newton" method and "modified Picard" method. Zarba, R.L. [14] used the modified Picard iteration method with both finite difference and finite element approximation in space. Ross et al.[15] used the Kirchhoff transformation to simulate water flow. Gottardi and Venutelli [16] presented a computer program, which integrates the three standard form of Richards equation using finite difference and finite element method. Huang et al. [17] proposed a new convergence criterion for the modified Picard iteration method. Gottardi et al. [18] used moving finite element model for one-dimensional solution. The stability analysis of fully implicit finite element scheme with Kirchhoff transform to this equation in Radu et al. [19] and a linearized finite difference scheme is presented in [20] also a numerical solution of Richards equation: a simple method adaptable in parallel computing is studied in [21]. An explicit stabilized Runge - Kutta - Legendre Super time - stepping scheme for the solution of Richards equation is studied in [22].

In this paper, we use Kirchhoff integral transform to reduce the highly nonlinear equation to a functional linear parabolic equation and solve it numerically.

The purpose of this paper is to present a reliable and accurate numerical scheme which is able to solve the two dimensional Kirchhoff transformed Richards equation, where numerical solution converges rapidly to the theoretically correct solution. The numerical solution is able to handle a short duration of infiltration and is relatively easier to implement.

This paper is organized as follows: In section 3, we present Kirchhoff transformation to (spatially) linearize the Richards equation. In section 4, we present the numerical methods based on finite difference method (CN). In section 5, we solve two test examples and compare the results. Finally in section 6, we conclude our results.

## 3. MODEL DESCRIPTION

We consider Richards equation (1.1), a diffusion process taking place in a vertical ditch with radius  $r$ . We assume axi - symmetry such that  $\theta$  is just a function of  $r, \vartheta, z$  and  $t$ ,  $r$  and  $z$  being the radial distance and axial distance from the center axis of the ditch to a point. For axi - symmetry, we take the cylindrical coordinates,  $r, \vartheta, z$  where  $z$  is the axial

direction and  $(r, \vartheta)$  are the polar coordinates in a cross section. From the relation  $x = r \cos \vartheta$ ,  $y = r \sin \vartheta$  and  $z = z$ , Richards equation as cylindrical coordinates, in axi symmetry form is:

$$(3.1) \quad \frac{\partial \theta}{\partial t} = \frac{1}{r} \frac{\partial}{\partial r} \left( r K(\psi) \frac{\partial \psi}{\partial r} \right) + \frac{\partial}{\partial z} \left( K(\psi) \frac{\partial \psi}{\partial z} \right) - \frac{\partial K(\psi)}{\partial z}$$

where  $r$  and  $z$  represent radial and axial direction respectively.

Richards equation (3.1) is typically used to simulate infiltration experiments (in both laboratory and field scale). These experiments begin in a cylindrical ditch with a dry soil and then water is poured on top of the ground surface, showing a clear connection with the Darcy's law. We assume that the infiltration with known surface flux does not exceed the infiltration intensity, and does not generate runoff. That is, we use the following initial and boundary conditions.

$$(3.2) \quad \begin{cases} \psi(r, z, 0) = \psi_0(r, z), & R_{in} \leq r \leq R_{out}, & 0 \leq z \leq Z_{top} \\ K(\psi) - K(\psi) \frac{\partial \psi}{\partial z} = q(t), & r > 0 & z = 0, & t > 0 \\ \psi(r, Z_{bot}, t) = \beta(t), & r > 0, & t > 0 \\ \frac{\partial \psi}{\partial r} = 0, & r = R_{out}, & z > 0, & t > 0 \\ \psi(R_{in}, Z, t) = \beta_1(t), & t > 0. \end{cases}$$

**3.1. Kirchhoff Integral Transform.** We use Kirchhoff integral transformation in equation (3.1), for this, we let  $h = \psi - z$  and define

$$(3.3) \quad \phi(h) = \int_0^h \bar{K}(\lambda) d\lambda.$$

Since  $K(h) > 0$  from (1.2), the function  $\phi(h)$  is strictly increasing with  $\bar{K}(h) = K(\psi)$ . Taking derivative of both sides of the transformation with respect to  $r$  and  $z$ , we obtain:

$$(3.4) \quad \frac{\partial \phi}{\partial r} = \frac{\partial \phi}{\partial h} \frac{\partial h}{\partial r} = \bar{K}(h) \frac{\partial(\psi - z)}{\partial r} = \bar{K}(h) \frac{\partial \psi}{\partial r} = K(\psi) \frac{\partial \psi}{\partial r}.$$

Again taking derivative of (3.4) with respect to  $r$ ,

$$(3.5) \quad \frac{\partial^2 \phi}{\partial r^2} = \frac{\partial}{\partial r} \left( K(\psi) \frac{\partial \psi}{\partial r} \right)$$

and

$$(3.6) \quad \frac{\partial \phi}{\partial z} = \frac{\partial \phi}{\partial h} \frac{\partial h}{\partial z} = \bar{K}(h) \frac{\partial(\psi - z)}{\partial z} = K(\psi) \left( \frac{\partial \psi}{\partial z} - 1 \right) = K(\psi) \frac{\partial \psi}{\partial z} - K(\psi)$$

Again differentiating of equation (3.6),

$$(3.7) \quad \frac{\partial^2 \phi}{\partial z^2} = \frac{\partial \left( K(\psi) \frac{\partial \psi}{\partial z} \right)}{\partial z} - \frac{\partial}{\partial z} (K(\psi)).$$

Using the equations (3.4), (3.5) and (3.7), the Richards equation (3.1), takes the form

$$(3.8) \quad \frac{\partial \theta}{\partial t} = \frac{\partial^2 \phi}{\partial r^2} + \frac{1}{r} \left( \frac{\partial \phi}{\partial r} \right) + \frac{\partial^2 \phi}{\partial z^2}$$

with  $\bar{\theta}(\phi) = \theta(h)$ . The corresponding initial and boundary conditions for the transformed equation (3.8) take the following form

$$(3.9) \quad \begin{cases} \phi(r, z, 0) = \phi_0(r, z), & R_{in} \leq r \leq R_{out} \quad 0 \leq z \leq Z_{top} \\ \frac{\partial \phi}{\partial z} = \bar{q}(t), & r > 0 \quad z = 0, \quad t > 0 \\ \phi(r, Z_{bot}, t) = \bar{\beta}(t), & r > 0, \quad t > 0 \\ \frac{\partial \phi}{\partial r} = 0, & r = R_{out}, \quad z > 0, \quad t > 0 \\ \phi(R_{in}, Z, t) = \bar{\beta}_1(t), & t > 0 \end{cases}$$

The Kirchhoff transformation transformed the nonlinear equation (3.1) to a nonlinear parabolic equation (3.8). Also we note that the Kirchhoff transformation preserves the uniqueness of the solution for the transformed problem.

#### 4. NUMERICAL METHOD

We have the transformed equation is in two different state variables. To solve the transformed equation (3.8) numerically with the prescribed initial and boundary conditions (3.9), it is feasible to have a single state variable. For this,  $\theta$  and  $\phi$  are assumed as single valued continuous functions of one another, and arranging these variables as

$$(4.1) \quad \frac{\partial \theta}{\partial t} = \frac{\partial \theta}{\partial \phi} \frac{\partial \phi}{\partial t} = \left( \frac{1}{\frac{\partial \phi}{\partial \theta}} \right) \frac{\partial \phi}{\partial t}, \quad \frac{\partial \phi}{\partial \theta} = \frac{\partial \phi}{\partial h} \frac{\partial h}{\partial \theta}.$$

Differentiating (1.2) with respect to  $h$ , we get

$$(4.2) \quad \frac{\partial \theta}{\partial h} = \alpha(\theta_s - \theta_r)(\alpha + |h|^\beta)^{-2} \cdot \beta |h|^{\beta-1}, \quad \frac{\partial \phi}{\partial h} = \bar{K}(h) = K(\psi).$$

Using (4.1) and (4.2), the transformed Richards equation (3.8) takes the form:

$$(4.3) \quad c(\phi) \frac{\partial \phi}{\partial t} = \frac{\partial^2 \phi}{\partial r^2} + \frac{1}{r} \frac{\partial \phi}{\partial r} + \frac{\partial^2 \phi}{\partial z^2},$$

where the functional coefficient  $c$  depends on  $\phi$  through  $h$  as

$$(4.4) \quad c(\phi(h)) = \frac{\alpha \beta (\theta_s - \theta_r) |h|^{\beta-1}}{\bar{K}(h) (\alpha + |h|^\beta)^2}.$$

**4.1. Finite Difference Discretization.** We set up a two dimensional  $(r, z)$  uniform grid for an axi-symmetric problem in the cylinder geometry by subdividing the radial length  $[R_n, R_{out}]$  into  $M_r$  subintervals of width  $\Delta r = \frac{R_{out} - R_{in}}{M_r}$  and the height  $[0, Z_{top}]$  into  $M_z$  subintervals of width  $\Delta z = \frac{Z_{top}}{M_z}$ . We construct a grid  $(r_i, z_j, t_n)$  with  $r_i = i \Delta r, i =$

$0, 1, 2, \dots, M_r$ ,  $z_j = j\Delta z, j = 0, 1, 2, \dots, M_z$ , and  $t_n = n\Delta t, n = 1, 2, \dots, N$ . Let  $\phi_{i,j}^n$  denote  $\phi(r_i, z_j, t_n)$ . The partial differential equation (4.3) can be approximated using forward difference in time and central difference in space as [23]

$$(4.5) \quad \left. \frac{\partial \phi}{\partial t} \right|_{(r_i, z_j, t_n)} \approx \frac{\phi_{i,j}^{n+1} - \phi_{i,j}^n}{\Delta t}, \quad \left. \frac{\partial \phi}{\partial r} \right|_{(r_i, z_j, t_n)} \approx \frac{\phi_{i+1,j}^n - \phi_{i-1,j}^n}{2\Delta r}.$$

$$\left. \frac{\partial^2 \phi}{\partial r^2} \right|_{(r_i, z_j, t_n)} \approx \frac{\phi_{i-1,j}^n - 2\phi_{i,j}^n + \phi_{i+1,j}^n}{\Delta r^2}, \quad \left. \frac{\partial^2 \phi}{\partial z^2} \right|_{(r_i, z_j, t_n)} \approx \frac{\phi_{i,j-1}^n - 2\phi_{i,j}^n + \phi_{i,j+1}^n}{\Delta z^2}$$

using a weighted average of the derivatives  $(\frac{\partial \phi}{\partial r}, \frac{\partial^2 \phi}{\partial r^2}, \frac{\partial^2 \phi}{\partial z^2})$  at a two time levels,  $t_n$  and  $t_{n+1}$  using Crank - Nicolson (CN) scheme equation (4.3) can be discretized as

$$(4.6) \quad \frac{\phi_{i,j}^{n+1} - \phi_{i,j}^n}{\Delta t} = \frac{1}{2c_{i,j}^n (\Delta r)^2} \left[ \phi_{i-1,j}^{n+1} - 2\phi_{i,j}^{n+1} + \phi_{i+1,j}^{n+1} + \phi_{i-1,j}^n - 2\phi_{i,j}^n + \phi_{i+1,j}^n \right]$$

$$+ \frac{1}{2c_{i,j}^n (\Delta z)^2} \left[ \phi_{i,j-1}^{n+1} - 2\phi_{i,j}^{n+1} + \phi_{i,j+1}^{n+1} + \phi_{i,j-1}^n - 2\phi_{i,j}^n + \phi_{i,j+1}^n \right]$$

$$+ \frac{1}{4r_i c_{i,j}^n (\Delta r)} \left[ \phi_{i+1,j}^{n+1} - \phi_{i-1,j}^{n+1} + \phi_{i+1,j}^n - \phi_{i-1,j}^n \right]$$

We collect the unknowns on the left hand side:

$$(4.7) \quad -\left(F_r - \frac{F}{r_i}\right)\phi_{i-1,j}^{n+1} + (1 + 2F_r + 2F_z)\phi_{i,j}^{n+1} - \left(F_r + \frac{F}{r_i}\right)\phi_{i+1,j}^{n+1} - F_z(\phi_{i,j-1}^{n+1} + \phi_{i,j+1}^{n+1})$$

$$= \left(F_r - \frac{F}{r_i}\right)\phi_{i-1,j}^n + (1 - 2F_r - 2F_z)\phi_{i,j}^n + \left(F_r + \frac{F}{r_i}\right)\phi_{i+1,j}^n - F_z(\phi_{i,j-1}^n + \phi_{i,j+1}^n),$$

where  $F_r = \frac{\Delta t}{2c_{i,j}^n (\Delta r)^2}$ ,  $F_z = \frac{\Delta t}{2c_{i,j}^n (\Delta z)^2}$ ,  $F = \frac{\Delta t}{4c_{i,j}^n (\Delta r)}$ .

Stability analysis of this equation (4.7) can be found in our previous work Timsina, R.C. et al. [22]. The equation (4.7) are coupled at the new time level  $n + 1$ . That is, we must solve a system of (linear) algebraic equations, which we will write as  $Bc = d$ , where  $B$  is the coefficient matrix,  $c$  is the vector of unknowns,  $d$  is the right hand-side.

To solve the above system of linear equations, we have a matrix system  $Bc = d$ , where the solution vector  $c$  must have one index. For this, we need a numbering of the unknowns with one index, not two as used in the mesh. We introduce a mapping  $position(i, j) = v(i, j)$  from a mesh point with indices  $(i, j)$  to the corresponding unknown  $u$  in the equation system.

$$u = v(i, j) = j(V_r + 1) + i, \text{ for } i = 0, 1, 2, \dots, V_r, j = 0, 1, 2, \dots, V_z,$$

With this mapping, we number the points along the radial direction starting with  $z = 0$  and then filled one mesh line at a time. In another way

$$u = v(i, j) = i(V_z + 1) + j, \text{ for } i = 0, 1, 2, \dots, V_r, j = 0, 1, 2, \dots, V_z.$$

with  $r = 0$  and then filled one mesh line at a time. From this we can get the general feature of the coefficient matrix obtained from the discretized equation (4.7).

Now  $B_{u,\nu}$  be the value of element  $(u, \nu)$  in the coefficient matrix  $B$ , where  $u$  and  $\nu$  are the numbering of the unknowns in the equation system. The then  $B_{u,u} = 1$  for  $u = \nu$  corresponding to the all known boundary values.  $u$  be  $v(i, j)$ , i.e., the single index

corresponding to the mesh point  $(i, j)$ . Then, for interior mesh along with boundary, we have

$$\begin{aligned} B_{v(i,j),v(i,j)} &= B_{u,u} = 1 + (F_r + F_z), \\ B_{u,v(i-1,j)} &= B_{u,u-1} = -F_r, \\ B_{u,v(i+1,j)} &= B_{u,u+1} = -F_r \\ B_{u,v(i,j-1)} &= B_{u,u-(V_z+1)} = -F_z \\ B_{u,v(i,j+1)} &= B_{u,u+(V_z+1)} = -F_z. \end{aligned}$$

The corresponding right hand side vector in the equation system has the entries  $d_u$ , where  $P$  numbers the equations with the given boundary values.

The above mention algorithm can be used to update the transformed variable  $\phi_{i,j}^n$  to its value in the next time level  $\phi_{i,j}^{n+1}$ . But we cannot advance the algorithm to the next time level  $\phi_{i,j}^{n+2}$  without evaluating the function  $c(\phi_{i,j}^{n+1})$  which requires computing the intermediate variable  $h_{i,j}^{n+1}$ . For this, we employ the equation (4.2) which can be approximated as

$$(4.8) \quad h_{i,j}^{n+1} = h_{i,j}^n + \frac{\phi_{i,j}^{n+1} - \phi_{i,j}^n}{\bar{K}(h_{i,j}^n)}.$$

## 5. SIMULATION RESULTS

**5.1. Experimental Setup.** The numerical procedure developed in the previous section is written in python and ran on a laptop with 2.8 GHz Quad-Core Intel Core i7 processor. We considered two specific infiltration experiments and inspect the behavior of the numerical scheme presented above. For the first case the setup consisted of an annulus ditch having length 70 cm in the axial direction and 100 cm in radial direction. The annulus was filled completely with sandy soil. We use the soil parameters and characteristics relationship between the soil moisture content  $\theta(\psi)$  and the hydraulic conductivity  $K(\psi)$  from the work of Haverkamp et al.[2].

$$(5.1) \quad \begin{aligned} K(\psi) &= K_s \frac{A}{\alpha + |\psi|^\gamma} = \frac{34 \times 1.175 \times 10^6}{1.175 \times 10^6 + |\psi|^{4.74}} \\ \theta(\psi) &= \theta_r + \frac{\alpha(\theta_s - \theta_r)}{\alpha + |\psi|^\beta} = 0.075 + \frac{1.611 \times 10^6 \times (0.287 - 0.075)}{1.611 \times 10^6 + |\psi|^{3.96}} \end{aligned}$$

The simulation starts with a uniform saturation  $\theta = 0.1 \text{ cm}^3/\text{cm}^3$  and a constant water head  $\psi = -61.5 \text{ cm}$  is maintained at the bottom boundary  $z = Z_{bot}$ . For the upper boundary  $z = Z_{top}$  at the soil surface, a constant flux  $q(t) = 13.69 \text{ cm/hr}$  for  $t < 0.7 \text{ hr}$  and zero normal flux condition for  $t > 0.7 \text{ hr}$  and for curved surface of the annulus zero flux boundary condition is maintained. For second case we considered that the same wetting flux for  $r > \frac{r}{2}$  and a constant drainage flux  $q(t) = -0.0099 \text{ cm/hr}$  for  $r < \frac{r}{2}$ . To compute the approximate solution using the Crank-Nicolson scheme, we have used a uniform spatial step size  $\Delta z = 2 \text{ cm}$  on axial direction and a step size of  $\Delta z = 2 \text{ cm}$  on radial direction and the simulation was run for 0.75 hr.

**5.2. Result and Discussion.** The Kirchoff transformed one dimensional model was employed to simulate vertical water infiltration into an unsaturated homogeneous porous medium. Numerical experiments were carried out by using sand column (proposed by Haverkamp et al.) with finite difference schemes (FTCS, BTCS, CN and RKL). Since we do not have exact solution we use numerical solution obtain from above (RKL) finite difference scheme for one dimensional as the reference solution Timsina, R. C. et al. [22] for numerical experiment of two dimensional water infiltration. Fig. (1) shows the variation of volumetric moisture content in sand for one dimension, as discussed in [22]. In this numer-

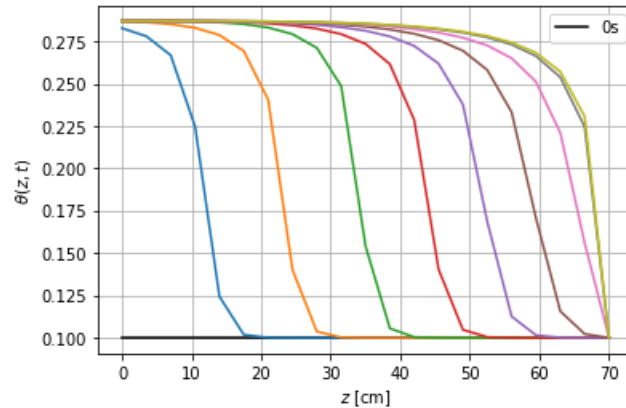


FIGURE 1. Variational trend of moisture content in depth (one dimension case)

ical experiment, the functions used for the hydraulic conductivity and the water content as in one dimensional case were taken from Haverkamp et al. [2]

The first two dimensional example is an unsaturated flow into a region of sandy soil. For this we suppose the domain is specified to be an annulus,  $r_{inner} \leq r \leq r_{outer}$  with  $r_{inner}$  strictly greater than zero, other than a disk. The annular domain consists of 70 cm in length with 100 cm of annular radius. We suppose it vertically downward where  $z$  axis taken as downward positive with a constant water head  $\psi = -61.5\text{cm}$  at left (Dirichlet) boundary condition  $r = R_{in}$  as dummy. A constant flux boundary condition (Neumann) on the right  $r = R_{out}$  is taken and a constant water head  $\psi = -61.5\text{ cm}$  at the bottom boundary  $z = Z_{bottom}$ . At the upper boundary  $z = 0$  (the soil surface), a constant flux  $q(t) = 13.69\text{ cm/hr}$  for  $t < 0.7\text{hr}$  and zero normal flux condition for  $t > 0.7\text{hr}$ . The solution domain was meshed using a spatial step size of  $\Delta z = 2\text{cm}$  on axial direction and a step size of  $\Delta r = 2.5\text{ cm}$  on radial direction and the simulation was run for 1 hr. The longitudinal water contain profiles and radial water contain profiles at time 0 hr and some others time are shown in figure (2)top. From this figure it is possible to note that the residual water contain at the bottom of the annulus is reached when time  $t$  is about .50 hr The moisture content contours are shown in figure (4)and corresponding surface plots of moisture content is in figure (3) left.

For the second example we considered the annulus with same dimensions and the numerical set up are the same for inner, outer and bottom of the domain. But, at the



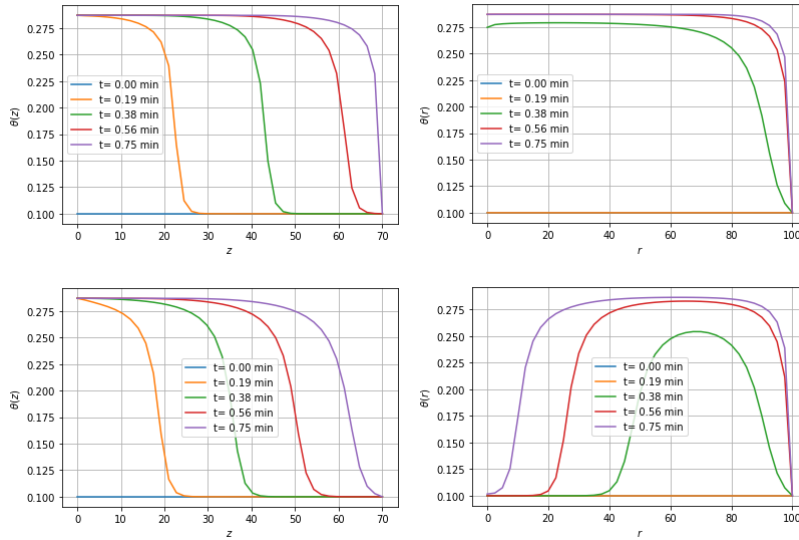


FIGURE 2. Longitudinal profile of soil moisture  $\theta(z)$  at  $r= 50$  cm(top left), radial profile of soil moisture  $\theta(z)$  at  $z= 35$  cm(top right), Longitudinal profile of soil moisture  $\theta(z)$  at  $r= 25$  cm(bottom left), radial profile of soil moisture  $\theta(z)$  at  $z= 35$  cm(bottom right)

top, i.e., on the soil surface we make a constant flux of drainage  $q(t) = -0.0099\text{cm/hr}$  for  $t < 0.7\text{hr}$  and zero normal flux condition for  $t > 0.7\text{hr}$  in half of the domain (for  $r = \frac{r}{2}$ ) and for the rest a constant flux of  $q(t) = 13.69\text{cm/hr}$  for  $t < 0.7\text{hr}$  and zero normal flux condition for  $t > 0.7\text{hr}$ . The longitudinal water contain profiles and radial water contain profiles at time 0 hr and some others time are shown in figure (2) bottom. From this figure it is possible to note that the residual water contain at the bottom of the annulus is reached when time  $t$  is about .30 hr for inner half circular part of the annulus. The moisture content contours are shown in figure (3) left and corresponding surface plots of moisture content are shown in figure (5).

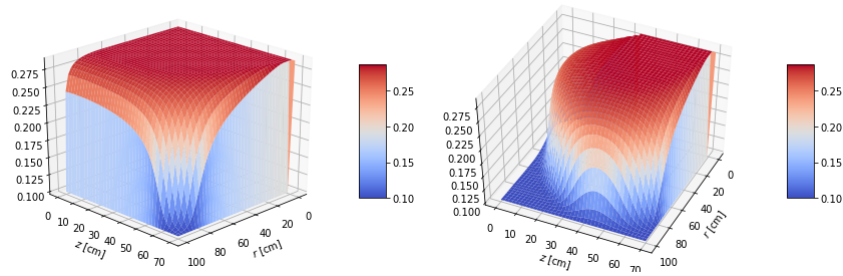


FIGURE 3. Soil Moisture  $\theta(r, z)$  at  $t = 0.75\text{sec}$  for  $r = R_{out}$ (left), Soil Moisture  $\theta(r, z)$  at  $t = 0.75\text{sec}$  for  $r = R_{out}/2$ (right)

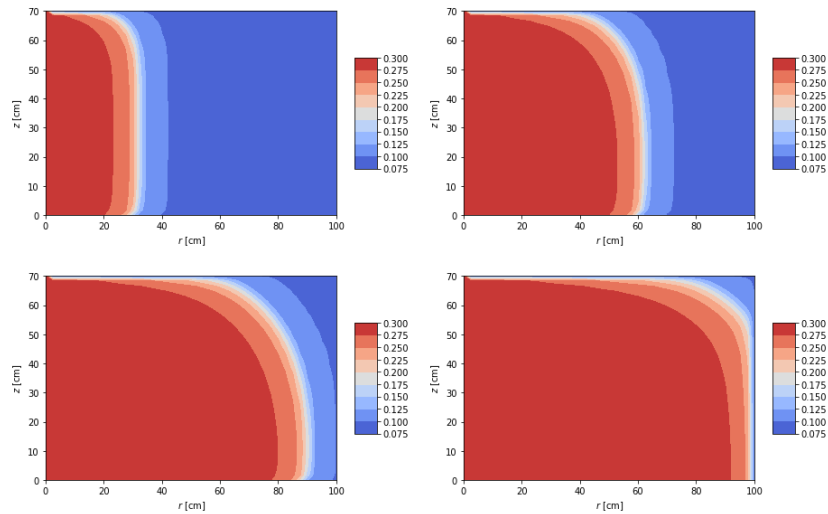


FIGURE 4. Soil Moisture  $\theta(r, z)$  at  $t = 0.1875\text{sec}$  for  $r = R_{out}$  (top left), Soil Moisture  $\theta(r, z)$  at  $t = 0.375\text{sec}$  for  $r = R_{out}$  (top right), Soil Moisture  $\theta(r, z)$  at  $t = 0.5625\text{sec}$  for  $r = R_{out}$  (bottom left), Soil Moisture  $\theta(r, z)$  at  $t = 0.75\text{sec}$  for  $r = R_{out}$  (bottom right)

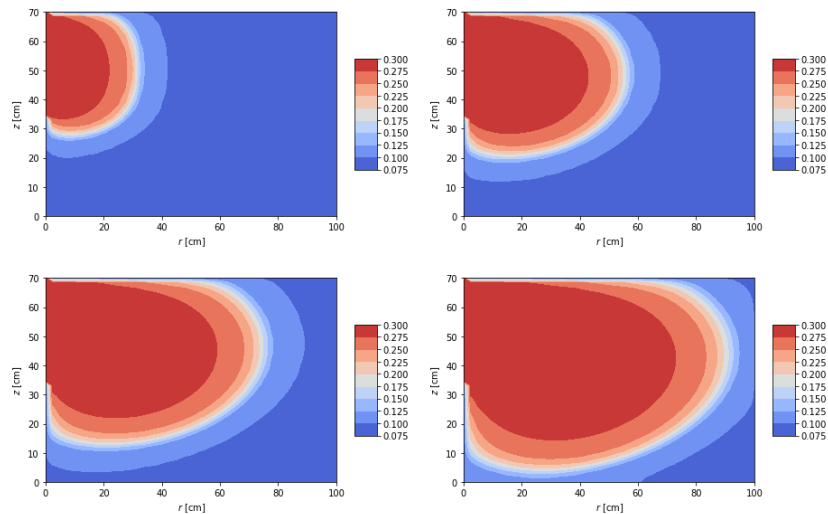


FIGURE 5. Soil Moisture  $\theta(r, z)$  at  $t = 0.1875\text{sec}$  for  $r = R_{out}/2$  (top left), Soil Moisture  $\theta(r, z)$  at  $t = 0.375\text{sec}$  for  $r = R_{out}/2$  (top right), Soil Moisture  $\theta(r, z)$  at  $t = 0.5625\text{sec}$  for  $r = R_{out}/2$  (bottom left), Soil Moisture  $\theta(r, z)$  at  $t = 0.75\text{sec}$  for  $r = R_{out}/2$  (bottom right)

## 6. CONCLUSION

In this work, we considered two dimensional Richards equation (a highly nonlinear degenerate parabolic partial differential equation) and solved it numerically. Also this work is based on two illustrative numerical examples in two dimension, with realistic parameters. We implemented Crank - Nicolson finite difference scheme. The work presented here

describes and verifies the employment and accuracy of Crank–Nicolson scheme to simulate flow in unsaturated porous media in axi symmetrical cylindrical sand ditch. However, this work presented a versatile numerical model which was able to solve the two dimensional Richards equation and the findings are converges to the theoretical analysis also the findings are in line with one dimensional approaches [22]. Figures 1 and 2 depicted that the numerical simulations results for the same infiltration experiment as in one dimension imposing, zero flux boundary conditions in the lateral boundary mimic the results from the one dimensional model. That is the longitudinal profile are in line with that of the one dimensional model. The numerical method was able to handle short duration infiltration and was relatively easy to implement. This work can be extended to achieve to accurate solution to heterogeneous soils with abruptly changing wetness conditions.

### Data Availability

The data used for supporting the findings of this study are included within the article.

### Conflicts of Interest

The author declares that there is no conflict of interest.

### REFERENCES

- [1] L. A. Richards, Capillary conduction of liquids through porous mediums, *Physics 1*, (5), 318-333, 1931.
- [2] R. Haverkamp, M. Vauclin, J. Touma, P. J. Wierenga, G. Vachaud, A comparison of numerical simulation models for one-dimensional infiltration, *Soil Sci. Soc. Am. J.*, 41(2), 285 – 294, 1997.
- [3] M. Th. Van Genuchten, E . A. Sudicky, Recent Advances in Vadose Zone flow and transport modeling, Vadose Zone Hydrology cutting across disciplines, *Oxford University Press*, 155-193, 1999.
- [4] M. A. Celia, E. T. Bouloutas, A General Mass-Conservative Numerical solution for the Unsaturated flow equation, *Water Resource research*, 26, 1483-1490, 1990.
- [5] D. R. Nielsen, M.T. van Genuchten, J.W. Biggar, Water Flow and Solute Transport Processes in the Unsaturated Zone, *Water Resour. Res.*, 22(9), pp 89 - 108, 1986.
- [6] P. C. D. Milly, Advances in Modeling of Water in the Unsaturated zone, *Transp. Porous Media*, 3, pp 491-514, 1988.
- [7] R. A. Frezze, Three-Dimensional, Transient, Saturated-Unsaturated Flow in a Groundwater Basin, *Water Resour. Res.*, Vol. 7, No. 2, pp 347-366, 1971.
- [8] T. N. Narasimhan, P. A. Witherspoon, An Integrated Finite Difference Method for Analyzing Fluid Flow in Porous Media, *Water Resour. Res.*, Vol. 12, pp 57-64, 1976.
- [9] S. P. Neuman, Saturated-unsaturated Seepage by Finite Elements, *J. Hydraul. Div. Am. Civ. Eng.*, Vol. 99, No. HY12, pp 2233-2250, 1973.
- [10] H. N. Hayhoe, Study of the Relative Efficiency of Finite Difference and Galerkin Techniques for Modeling Soilwater Transfer, *Water Resour. Res.*, Vol. 14, 97-102, 1978.
- [11] P. S. Huyakorn, S. D. Thomas, B. M. Thompson, Techniques for Making Finite Elements Competitive in Modeling Flow in Variably Saturated Media, *Water Resour. Res.*, Vol. 20, pp 1099-1115, 1984.
- [12] M. T. van Genuchten, A Closed-form Equation for Predicting the Hydraulic Conductivity of Unsaturated Soils, *Soil Sci. Soc. Am. J.*, Vol. 44, No. 5, pp 892-898, 1980.
- [13] M. B. Allen, Murphy, A Finite Element Collocation Method for Variable Saturated Flow in Two Dimensions, *Water Resour. Res.*, Vol. 22, pp 1537-1542, 1996.
- [14] R. L. Zarba, A Numerical Investigation of Unsaturated Flow, *M.S. Thesis, Dep. of Civ. Eng., Mass. Inst. of Technol., Cambridge*, 1988.
- [15] P. J. Ross, K. L. Bristow, Simulating Water Movement in Layered and Gradational Soils using the Kirchhoff Transform, *Soil Sci. Soc. Am. J.*, Vol. 54, pp 1519-1524, 1990.

- [16] G. Gottardi, M. Venuteli, Richards: Computer Programming for the numerical simulation of one-dimensional infiltration into unsaturated soil, *Computers and Geo-sciences*, 19, 1239-1266, 1993.
- [17] K. Huang, B. P. Mohanty, M. T. van Genuchten, A New Convergence Criterion for the Modified Picard Iteration Method to Solve the Variably Saturated Flow Equation, *J. Hydrol.*, Vol. 178, pp 69-91, 1996.
- [18] G. Gottardi, M. Venuteli, Moving Finite Element Model for one-dimensional infiltration into unsaturated soil, *Water Resource Research*, vol-28, 3259-3267, 1992.
- [19] F. A. Radu, L. Florian, A Study on iterative methods for solving Richards equation, *Computers and Geo-sciences*, 20,341-353, 2016.
- [20] F. Liu, Y. Fukumoto, X. Zhao, A linearized finite difference Scheme for the Richards equation under variable-Flux boundary conditions, *Journal of scientific computing*, 83, 2-21, 2020.
- [21] N. Egid, E. Gioia, P. Maponi, L. Spadoni., A numerical solution of Richards equation: a simple method adaptable in parallel computing, *International Journal of computer Mathematics*, 97, 2-17, 2020.
- [22] R. C. Timsina, H. Khanal, K. N. Uprety, An explicit stabilized Runge-Kutta-Legendre super time-stepping scheme for the Richards equation, *Mathematical problems in Engineering*, vol-2021, 1-11, 2021.
- [23] J. W. Thomas, Numerical partial differential equations: Finite difference methods, *Text in Applied Mathematics*, Springer, 2010.